on appropriate choices of time-discretization methods and time-step limits for temporal stability.

For the reader's convenience, Table D.1 provides the numerical values of the intersections of the absolute stability regions with the negative real axis and the positive imaginary axis for all methods discussed in this section.

D.2.1 Leap Frog Method

The *leap frog* (LF) method (also called *midpoint* method) is a second-order, two-step scheme given by

$$\mathbf{u}^{n+1} = \mathbf{u}^{n-1} + 2\Delta t \mathbf{f}^n \ . \tag{D.2.1}$$

This produces solutions of constant norm for the model problem provided that $\lambda\Delta t$ is on the imaginary axis and that $|\lambda\Delta t| \leq 1$ (see Table D.1). Thus, leap frog is a suitable explicit scheme for problems with purely imaginary eigenvalues. It also is a reversible, or symmetric, method. However, since it is only well-behaved on a segment in the complex $\lambda\Delta t$-plane for the model problem, extra care is needed in practical situations.

The most obvious application is to periodic advection problems, for the eigenvalues of the Fourier approximation to $\mathrm{d}/\mathrm{d}x$ are imaginary. The difficulty with the leap frog method is that the solution is subject to a temporal oscillation with period $2\Delta t$. This arises from the extraneous (spurious) solution to the temporal difference equations. The oscillations can be controlled by every so often averaging the solution at two consecutive time-levels.

Leap frog is quite inappropriate for problems whose spatial eigenvalues have nonzero real parts. This certainly includes the approximation of diffusion operators. Leap frog is also not viable for advection operators with nonperiodic boundary conditions, since the discrete spectra of Chebyshev and Legendre approximations to the standard advection operator have appreciable real parts.

D.2.2 Adams–Bashforth Methods

This is a class of explicit multistep methods which includes the simple *forward Euler* (FE) method

$$\mathbf{u}^{n+1} = \mathbf{u}^n + \Delta t \mathbf{f}^n \ , \tag{D.2.2}$$

the popular *second-order Adams–Bashforth* (AB2) method

$$\mathbf{u}^{n+1} = \mathbf{u}^n + \tfrac{1}{2}\Delta t \left[3\mathbf{f}^n - \mathbf{f}^{n-1}\right] \ , \tag{D.2.3}$$

the still more accurate *third-order Adams–Bashforth* (AB3) method

$$\mathbf{u}^{n+1} = \mathbf{u}^n + \tfrac{1}{12}\Delta t \left[23\mathbf{f}^n - 16\mathbf{f}^{n-1} + 5\mathbf{f}^{n-2}\right] \ , \tag{D.2.4}$$

and the *fourth-order Adams–Bashforth* (AB4) method

$$\mathbf{u}^{n+1} = \mathbf{u}^n + \tfrac{1}{24}\Delta t \left[55\mathbf{f}^n - 59\mathbf{f}^{n-1} + 37\mathbf{f}^{n-2} - 9\mathbf{f}^{n-3}\right] . \qquad \text{(D.2.5)}$$

These methods are not reversible.

The stability regions $\mathcal{A}$ of these methods are shown in Fig. D.1 (left) and the stability boundaries along the axes are given in Table D.1. Note that the size of the stability region decreases as the order of the method increases. Note also that except for the origin, no portion of the imaginary axis is included in the stability regions of the first and second-order methods, whereas the third- and fourth-order versions do have some portion of the imaginary axis included in their stability regions. Nevertheless, the AB2 method is weakly unstable, i.e., for a periodic, hyperbolic problem the acceptable Δt decreases at T increases.

As is evident from Fig. D.1 (left), higher order AB methods are temporally stable for Fourier approximations to periodic advection problems. Let the upper limit of the absolute stability region along the imaginary axis be denoted by c. Then the temporal stability limit is

$$\frac{N}{2}\Delta t \le c\,, \qquad \text{or} \qquad \Delta t \le \frac{c}{\pi}\,\Delta x\,. \qquad \text{(D.2.6)}$$

The limit on Δt is smaller by a factor of π than the corresponding limit for a second-order finite-difference approximation in space. The Fourier spectral approximation is more accurate in space because it represents the high-frequency components much more accurately than the finite-difference method. The artificial damping of the high-frequency components which is produced by finite-difference methods enables the stability restriction on the time-step to be relaxed.

Chebyshev and Legendre approximations to advection problems appear to be temporally stable under all Adams–Bashforth methods for sufficiently small Δt; precisely, for $\Delta t \le CN^{-2}$ for a suitable constant C. (For simplicity, this and the subsequent stability limits refer to a single-domain discretization. For multidomain methods, the limits on Δt should also scale with the size of the subdomains, in a way that depends on the specific spatial discretization method that is being used). Since the spatial eigenvalues all have negative real parts, the failure of the AB2 method to include the imaginary axis in its absolute stability region does not preclude temporal stability.

The temporal stability limits for Adams–Bashforth methods for Fourier, Chebyshev and Legendre approximations to diffusion equations are easy to deduce since their spatial eigenvalues (i.e., the eigenvalues of the matrix $-L$) are real, negative and limited in modulus as indicated, e.g., in CHQZ2, Chap. 4. Combining this information with the stability bounds along the negative real axis as provided in Table D.1, one gets that Δt should be limited by a constant times N^{-2} for Fourier approximations, by a constant times N^{-4} for Chebyshev or Legendre collocation approximations, and by a constant times N^{-3} for Legendre G-NI approximations.

D.2.3 Adams–Moulton Methods

A related set of implicit multistep methods are the Adams–Moulton methods. They include the *backward Euler* (BE) method

$$\mathbf{u}^{n+1} = \mathbf{u}^n + \Delta t \mathbf{f}^{n+1} \ , \tag{D.2.7}$$

the *Crank–Nicolson* (CN) method

$$\mathbf{u}^{n+1} = \mathbf{u}^n + \tfrac{1}{2}\Delta t[\mathbf{f}^{n+1} + \mathbf{f}^n] \ , \tag{D.2.8}$$

the *third-order Adams–Moulton* (AM3) method

$$\mathbf{u}^{n+1} = \mathbf{u}^n + \tfrac{1}{12}\Delta t[5\mathbf{f}^{n+1} + 8\mathbf{f}^n - \mathbf{f}^{n-1}] \ , \tag{D.2.9}$$

and the *fourth-order Adams–Moulton* (AM4) method

$$\mathbf{u}^{n+1} = \mathbf{u}^n + \tfrac{1}{24}\Delta t[9\mathbf{f}^{n+1} + 19\mathbf{f}^n - 5\mathbf{f}^{n-1} + \mathbf{f}^{n-2}] \ . \tag{D.2.10}$$

Forward Euler (FE) (see D.2.2), backward Euler (BE) and Crank–Nicolson (CN) methods are special cases of θ-methods, defined as

$$\mathbf{u}^{n+1} = \mathbf{u}^n + \Delta t[\theta \mathbf{f}^{n+1} + (1-\theta)\mathbf{f}^n] \ , \tag{D.2.11}$$

for $0 \le \theta \le 1$. Precisely, they correspond to the choice $\theta = 0$ (FE), $\theta = 1$ (BE) and $\theta = 1/2$ (CN). All θ-methods except for FE are implicit. All θ-methods are first-order accurate, except for CN, which is second-order. For each $\theta < \frac{1}{2}$, the absolute stability region is the circle in the left half-plane $Re(\lambda\Delta t) \le 0$ with center $z = (2\theta - 1)^{-1}$ and radius $r = (1 - 2\theta)^{-1}$. The stability region of the CN method coincides with the half-plane $Re(\lambda\Delta t) \le 0$. For each $\theta > \frac{1}{2}$, the absolute stability region is the exterior of the open circle in the right half-plane $Re(\alpha) > 0$ with center $z = (2\theta - 1)^{-1}$ and radius $r = (2\theta - 1)^{-1}$. Thus, all θ-methods for $\frac{1}{2} \le \theta \le 1$ are A-stable.

The absolute stability regions of the third- and fourth-order Adams–Moulton methods are displayed in Fig. D.1 (right) and the stability boundaries along the axes are given in Table D.1. In comparison with the explicit Adams–Bashforth method of the same order, an Adams–Moulton method has a smaller truncation error (by factors of five and nine for second and third-order versions), a larger stability region, and requires one fewer levels of storage. However, it does require the solution of an implicit set of equations. The CN method is reversible; the others are not.

The CN method is commonly used for diffusion problems. In Navier–Stokes calculations, it is frequently applied to the viscous and pressure gradient components. Although CN is absolutely stable for the former and temporally stable for the latter, it has the disadvantage that it damps high-frequency components very weakly, whereas in reality these components decay very rapidly.

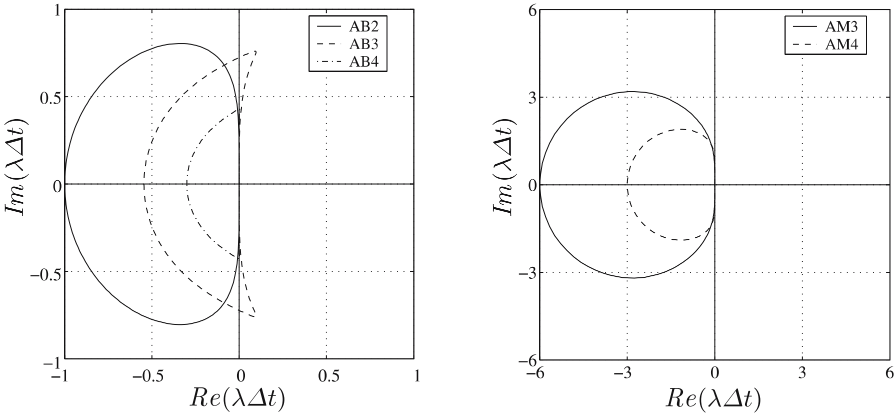

Fig. D.1. Absolute stability regions of Adams–Bashforth (*left*) and Adams–Moulton (*right*) methods

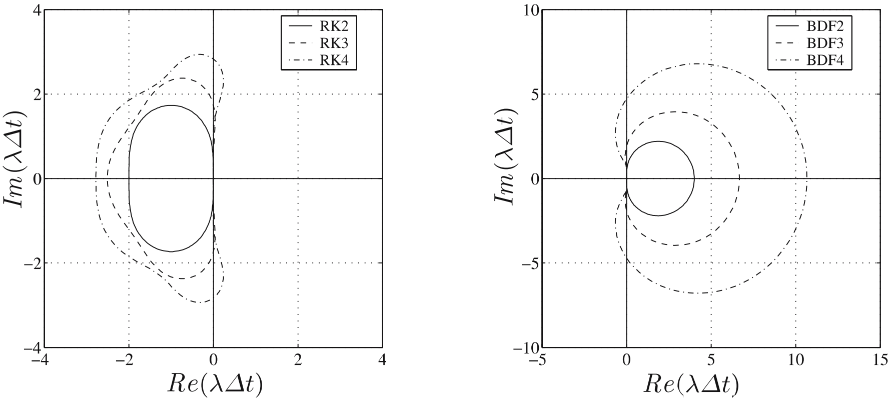

Fig. D.2. Absolute stability regions of backwards-difference formulas (*left*) and Runge–Kutta methods (*right*). The BDF methods are absolutely stable on the exteriors (and boundaries) of the regions enclosed by the curves, whereas the RK methods are absolutely stable on the interiors (and boundaries) of the regions enclosed by the *curves*

The Adams–Moulton methods of third and higher order are only conditionally stable for advection and diffusion problems. The stability limits implied by Fig. D.1 indicate that the stability limit of a high-order Adams–Moulton method is roughly ten times as large for a diffusion problem as the stability limit of the corresponding Adams–Bashforth method. In addition, AM3 and AM4 are weakly unstable for Fourier approximations to advection problems, since the origin is the only part of the imaginary axis which is included in their absolute stability regions.

Table D.1. Intersections of absolute stability regions with the negative real axis (*left*) and with the positive imaginary axis (*right*)

Method	$\mathcal{A} \cap \mathbb{R}_-$	$\mathcal{A} \cap i\mathbb{R}_+$
Leap frog (midpoint)	$\{0\}$	$[0, 1]$
Forward Euler	$[-2, 0]$	$\{0\}$
Crank–Nicolson	$(-\infty, 0]$	$[0, +\infty)$
Backward Euler	$(-\infty, 0]$	$[0, +\infty)$
θ-method, $\theta < 1/2$	$[2/(2\theta - 1), 0]$	$\{0\}$
θ-method, $\theta \geq 1/2$	$(-\infty, 0]$	$[0, +\infty)$
AB2	$(-1, 0]$	$\{0\}$
AB3	$[-6/11, 0]$	$[0, 0.723]$
AB4	$[-3/10, 0]$	$[0, 0.43]$
AM3	$[-6, 0]$	$\{0\}$
AM4	$[-3, 0]$	$\{0\}$
BDF2	$(-\infty, 0]$	$[0, +\infty)$
BDF3	$(-\infty, 0]$	$[0, 1.94)$
BDF4	$(-\infty, 0]$	$[0, 4.71)$
RK2	$[-2, 0]$	$\{0\}$
RK3	$[-2.51, 0]$	$[0, 1.73]$
RK4	$[-2.79, 0]$	$[0, 2.83]$

D.2.4 Backwards-Difference Formulas

Another class of implicit time discretizations is based upon backwards-difference formulas. These include the *first-order backwards-difference scheme* (BDF1), which is identical to backward Euler, the *second-order backwards-difference scheme* (BDF2)

$$\mathbf{u}^{n+1} = \tfrac{1}{3}[4\mathbf{u}^n - \mathbf{u}^{n-1}] + \tfrac{2}{3}\Delta t \mathbf{f}^{n+1} \ , \tag{D.2.12}$$

the *third-order backwards-difference scheme* (BDF3)

$$\mathbf{u}^{n+1} = \tfrac{1}{11}[18\mathbf{u}^n - 9\mathbf{u}^{n-1} + 2\mathbf{u}^{n-2}] + \tfrac{6}{11}\Delta t \mathbf{f}^{n+1} \ , \tag{D.2.13}$$

and the *fourth-order backwards-difference scheme* (BDF4)

$$\mathbf{u}^{n+1} = \tfrac{1}{25}[48\mathbf{u}^n - 36\mathbf{u}^{n-1} + 16\mathbf{u}^{n-2} - 3\mathbf{u}^{n-3}] + \tfrac{12}{25}\Delta t \mathbf{f}^{n+1} \ . \tag{D.2.14}$$

The absolute stability regions of these methods are displayed in Fig. D.2 (left), and the stability boundaries along the axes are given in Table D.1. The stability regions are much larger than those of the corresponding AM methods.